European Review for Medical and Pharmacological Sciences 2021; 25: 4372-4384

Mesenchymal stem cells derived from epicardial adipose tissue reverse cardiac remodeling in a rabbit model of myocardial infarction

B. ÖZKAYNAK[1], İ. ŞAHIN[2], E. ÖZENC[3], C. SUBAŞI[4], D.S. ORAN[5], T. TOTOZ[6], Ü.S. TETIKKURT[7], B. MERT[1], A. POLAT[1], E. OKUYAN[2], E. KARAÖZ[4,8,9]

[1]Cardiovascular Surgery Department, Bağcılar Training and Research Hospital, İstanbul, Turkey
[2]Cardiology Department, Bağcılar Training and Research Hospital, İstanbul, Turkey
[3]Cardiology Department, Liv Hospital, İstanbul, Turkey
[4]Department of Histology & Embryology, İstinye University, Faculty of Medicine, İstanbul, Turkey
[5]Experimental Research and Skills Development Center, Bağcılar Training and Research Hospital, İstanbul, Turkey
[6]Anaesthesiology and Reanimation Department, Bağcılar Training and Research Hospital, İstanbul, Turkey
[7]Department of Pathology, Bağcılar Training and Research Hospital, İstanbul, Turkey
[8]Center for Stem Cell and Tissue Engineering Research & Practice, İstinye University, İstanbul, Turkey
[9]Center for Regenerative Medicine and Stem Cell Manufacturing (LivMedCell), Liv Hospital, İstanbul, Turkey

Abstract. – OBJECTIVE: Myocardial infarction (MI) is one of the most important causes of death. MI-related tissue loss and cardiac remodeling may result in heart failure. Intramyocardial injection of mesenchymal stem cells derived from adipose tissues, in acute MI animal models, has shown promising regenerative capabilities. This study aimed to investigate the myocardial regenerative capacity of epicardial adipose tissue-derived mesenchymal stem cells (ADSCs) in a rabbit model of MI.

MATERIALS AND METHODS: A rabbit model of MI was performed in three groups: a sham-operated group, a control group, and a treatment group. MI was induced by coronary artery ligation via thoracotomy in the first operation. Four weeks after the first operation, intramyocardial injections of phosphate-buffered saline (PBS; control group) or ADSCs (10×10^6 in 100 µL; treatment group) were performed in the peri-infarct zone. Four weeks after the second operation, rabbits were sacrificed for further analysis.

RESULTS: A significant increase in ejection fraction ($p<0.0001$) was detected in the treatment group, along with a significant increase in vascular density ($p<0.001$) and a significant decrease in infarct size ($p<0.05$) compared to the control group.

CONCLUSIONS: Epicardial adipose tissue is a rich source of mesenchymal stem cells, which can differentiate into cardiomyocytes, as well as having neoangiogenic properties. Due to its potential to ameliorate chronic ischemic changes in the heart, it may be preferable in cardiac regenerative cell therapies.

Key Words:
Stem cell, Adipose-derived stem cells, Mesenchymal stem cells, Epicardial adipose tissue, Myocardial regeneration.

Introduction

Myocardial infarction (MI) is one of the leading causes of mortality and heart failure (HF). MI survivors risk progressing to HF, which is a major concern. After MI, several cytokines and growth factors induce inflammatory processes to increase tissue healing, but ischemic tissue is replaced by fibrotic scarring, which leads to cardiac remodeling. The size of the infarcted areas is related to the mortality rate[1]. Although many therapeutic options exist to manage HF, including revascularization and medical treatment and devices, none succeed in complete myocardial regeneration. The use of stem cell-based therapies, with a potential for regeneration, provides an attractive approach for cardiovascular diseases. Stem cell transplantation for regeneration of

Corresponding Author: Berk Özkaynak, MD; e-mail: berkozkaynak@gmail.com

heart tissue to enhance the recovery of ventricular function in MI raises hope for future treatment modalities.

Embryonic stem cells are pluripotent cells with teratogenic differentiation risks, but mesenchymal stem cells (MSCs) have shown promising results in this regard. Different tissue types have been studied as sources of MSCs, which can differentiate into various tissue cell types, including cardiomyocytes, endothelial cells, and smooth muscle cells[2-4]. Adipose tissue has been identified as a rich source of MSCs[5], but epicardial adipose tissue-derived mesenchymal stem cells (ADSCs) have a higher potency to differentiate compared to other adipose tissue sources[6,7]. This study investigated the myocardial regenerative capacity of epicardial ADSCs in a rabbit model of MI.

Materials and Methods

Animals

Twenty-five New Zealand White rabbits, each weighing between 3 and 3.5 kg, were used without exclusions in this experiment. All animals were bred and treated with maximum care at the Center for Experimental Research and Development of our institution, in accordance with Directive 2010/63/EU of the European Parliament and of the Council on the protection of animals used for scientific purposes and Commission Recommendation 2007/526/EC on guidelines for the accommodation and care of animals used for experimental and other scientific purposes. The experimental protocol was approved by the Local Ethics Committee for Animal Experiments at our institution (2011/16). The sample size in each group was chosen to use the smallest number of animals for statistical significance. Only the operators performing the echocardiographic and histopathological evaluations were blinded.

Study Design

Animals were randomly allocated into three groups.

1. Phosphate-buffered saline (PBS) group (placebo; n=10): The animals were operated to induce MI initially. After 4 weeks, a second operation was performed to apply intramyocardial PBS. PBS was the transport medium of the stem cells used in this study, and it was assigned as the control treatment. Four weeks after the second operation, the animals were sacrificed.
2. ADSC group (treatment; n=10): The animals were operated to induce MI initially. After 4 weeks, a second operation was performed to apply intramyocardial ADSCs. Four weeks after the second operation, the animals were sacrificed.
3. Sham-operated group (n=5): The animals were operated in the same way as the treatment groups but without inducing MI. After 4 weeks, a second operation was performed in the same way, but without applying any treatments. Four weeks after the second operation, the animals were sacrificed.

Assessment of Left Ventricle Function

Three investigations were performed for each animal: baseline (before the first operation), post-MI (before the second operation), and post-treatment (before sacrification). Echocardiographic evaluations were performed for each rabbit under mild sedation (2% isoflurane) before the day of each procedure.

All images were obtained with a Philips HD11XE ultrasound system and S 8-3 probe (Philips, Andover, MA, USA). Echocardiographic views were obtained from the right parasternal and left apical windows. Parasternal views were obtained with the rabbits placed in dorsal recumbency and the probe positioned with cranial angulation over a shaved area on the lower portion of the thoracic wall. The exact positioning of the transducer was adjusted as necessary to acquire the standard views. For apical views, the transducer was moved slightly caudally and angled cranially. Echocardiographic measurements using both 2D and M-modes were obtained in the parasternal right axis views. These included interventricular and left ventricular free-wall thickness in diastole and systole and left ventricular internal diameter at end diastole (LVIDd) and end systole (LVIDs). Fractional shortening was computed by using the equation [(LVIDd – LVIDs) / LVIDd] × 100%, and ejection fraction was calculated using the Teichholz formula[8]. The average of the three different measurements for each parameter, performed by an investigator blinded to the treatment group, was used for final outcome analysis.

Operations

MI was induced by permanent ligation of the left circumflex coronary artery as described previously[9]. Briefly, the rabbits were anesthetized with xylazine (5 mg/kg IM) and isoflurane (3-4%) at induction. Following endotracheal intubation, isoflurane (1–2%) was used for maintenance of

anesthesia while the respirator was set at 75 mL tidal volume with a frequency of 20 breaths per minute.

The heart was exposed through left lateral thoracotomy. The left circumflex coronary artery was identified below the left atrial appendage and ligated in the mid segment (around 10 to 15 mm from the apex) using 6/0 polypropylene suture. In the sham-operated animals (n=5), the heart was exposed through the left thoracotomy, but coronary ligation was not performed. Four weeks after the initial operation, left ventricle (LV) function was evaluated by echocardiography. Repeat left thoracotomy was performed. Intramyocardial injections of PBS (control group) or ADSCs (10×10^6 in 100 μL; treatment group) were performed in the peri-infarct zone (myocardium surrounding the necrotic area) using a 29-gauge needle. A total volume of 100 μL ADSCs or PBS was injected into all four quadrants of the peri-infarct border (4×25 μL). No injections were performed in the sham-operated rabbits. Four weeks after the final operation, echocardiographic evaluations were repeated in all the animals, and they were sacrificed using high-dose isoflurane.

Sacrification

The rabbits were anesthetized with xylazine (5 mg/kg IM) and isoflurane (5-10%). Median sternotomy was performed, opening the pericardium and both pleural spaces to expose the heart and the great vessels.

For effective internal and external fixation, in the beating heart, the ascending aorta was cross-clamped and the aortic root was perfused with neutral-buffered 10% formaldehyde solution, while draining blood from the right atrium and the pulmonary veins. After draining the whole blood, the heart was explanted and immersed in neutral-buffered 10% formaldehyde solution. Before paraffin-block preparation, the heart was macroscopically examined for scar formation, and sequential sagittal sections were obtained for paraffin processing.

Isolation and characterization of ADSCs

Isolation of ADSCs

ADSCs were isolated from epicardial fat using previously established methods[10-12]. Adipose tissue was washed thoroughly with PBS and then digested at 37°C for 1 hour (h) in an equal volume of 0.1% type I collagenase. The cell suspension was filtered using a 70-μm mesh nylon filter (Becton Dickinson Labware, Franklin Lakes, NJ, USA). The cells were resuspended in an L-Dulbecco's Modified Medium (DMEM) supplemented with 1% penicillin/streptomycin and 10% fetal bovine serum (FBS; standard culture medium). After centrifugation at 1,800 rpm for 10 minutes (min), the cells were cultured in a standard culture medium in 25 cm^2 culture flasks and incubated under standard conditions (37°C, 5% CO_2). After 5-7 days, the medium was replaced with fresh medium and subsequently replaced twice per week. After reaching 70-80% confluence, the cells were harvested with 0.025% trypsin-EDTA for 3-4 min, collected by centrifugation, and subcultured at a 1:3 ratio. The cells were counted using trypan blue (Biological Industries, Kibbutz Beit Haemek, Israel). The blue staining of cells after mixing (1:1) was used as an indicator of cell death.

Characterization of ADSCs

Flow cytometry: Undifferentiated ADSCs were subjected to flow cytometry analysis. After passage 3 (P3), stem cells were harvested. Flow cytometry was performed using a FACS™ Calibur (BD Biosciences, Franklin Lakes, NJ, USA). Immunophenotyping analysis was performed against the following antigens: CD44, CD45, CD90, CD105, major histocompatibility complex (MHC) class I, and MHC class II (BD Biosciences, San Jose, CA, USA). The data were analyzed with Cell Quest software (BD Biosciences, San Jose, CA, USA).

Immunohistochemistry: To identify cellular markers, P3 cells were seeded on poly-L-lysine-coated 8-well chamber slides (BD Biosciences, San Jose, CA, USA), cultured for another 1–2 days, and subjected to immunocytochemistry and immunofluorescence staining.

Immunofluorescence staining: samples were rinsed briefly in PBS, fixed in ice-cold methanol for 10 min, and then allowed to dry completely. After permeabilization with 0.025% Triton X-100 (Merck, Darmstadt, Germany), the cells were incubated with 1.5% normal goat or donkey blocking serum (Santa Cruz Biotechnology, Santa Cruz, CA, USA) in PBS for 30 min at 37°C to suppress non-specific binding of IgGs. After washing three times with PBS (5 min each), the cells were incubated overnight at 4°C with the primary antibodies alpha-smooth muscle actin (ASMA; Thermo Fisher Scientific, Branchburg, NJ, USA, catalog no: MS-113-P), cytokeratin 18

(Arigo Biolaboratories, Hsinchu City, Taiwan, catalog no: ARG62975), cytokeratin 19 (Merck Millipore, Darmstadt, Germany, catalog no: MAB1675), fibroblast growth factor (FGF; Santa Cruz Biotechnology, Santa Cruz, CA, USA, catalog no: SC-79), fibronectin (Santa Cruz Biotechnology, Santa Cruz, CA, USA, catalog no: SC-8422), glial fibrillary acidic protein (GFAP; Thermo Fisher Scientific, Branchburg, NJ, USA, catalog no: MS-280-P), vimentin (Santa Cruz Biotechnology, Santa Cruz, CA, USA, catalog no: SC-7557), and vinculin (Thermo Fisher Scientific, Branchburg, NJ, USA, catalog no: MS-1209-P). After three PBS washes, cells were incubated with FITC (Santa Cruz Biotechnology, Santa Cruz, CA, USA)-labeled appropriate secondary antibodies for 45 min in darkness. After washing three times with PBS, the cells were mounted with mounting medium containing DAPI (Santa Cruz Biotechnology, Santa Cruz, CA, USA).

Immunoperoxidase staining: Immunocytochemical analysis was performed using the streptavidin-peroxidase method (Thermo Scientific™ Lab Vision™ UltraVision™ Plus Large Volume Detection System: Anti-Polyvalent, HRP [Ready-To-Use] immunostaining kit, Thermo Fisher Scientific Anatomical Pathology, Runcorn, Cheshire, UK). To reduce nonspecific background staining due to endogenous peroxidase, cultured cells were fixed in ice-cold methanol with 0.3% hydrogen peroxide (Carlo Erba Reactifs, PA Des Portes, Val-De-Reuil, France) for 15 min and allowed to dry. After additional PBS washes, cells were incubated with Ultra V Block for 5 min at room temperature. Then, cells were incubated overnight at 4°C with the primary antibodies c-fos (Santa Cruz Biotechnology, Santa Cruz, CA, USA, catalog no: sc-52), Ki67 (Abcam, Cambridge, UK, catalog no: ab15580), osteonectin (Abcam, Cambridge, UK, catalog no: ab1858), and CD105 (Thermo Fisher Scientific, Branchburg, NJ, USA, catalog no: MS-1290-P). The next day, cells were incubated with biotinylated secondary antibodies for 15 min at room temperature. Incubation was followed by streptavidin-peroxidase treatment for 15 min at room temperature, and signals were detected with an AEC kit (Zymed® Laboratories, Invitrogen Ltd., Paisley, UK). The cells were counterstained with hematoxylin (Santa Cruz Biotechnology, Santa Cruz, CA, USA) and examined under a light microscope (Zeiss Axio Observer 1, Carl Zeiss Microscopy GmbH, Jena, Germany).

In vitro Differentiation of ADSCs

Adipogenic and osteogenic differentiations were performed *in vitro* according to a published protocol[13].

For osteogenic differentiation, the cells were incubated in standard culture medium supplemented with 100 nmol/mL dexamethasone, 0.05 mmol/mL ascorbate-2-phosphate, and 10 mmol/mL b-glycerophosphate for 4 weeks. Osteogenic differentiation was assessed via staining with 2% Alizarin Red S (pH 4.1-4.3; Sigma-Aldrich, St. Louis, MO, USA).

Adipogenic differentiation was performed by incubation of MSCs in standard culture medium supplemented with 0.5 mmol/mL isobutyl-methylxanthine, 10^{-6} M dexamethasone, 10 mg/mL insulin, and 200 mmol/mL indomethacin for 2 weeks. Adipogenic differentiation was shown by staining intracellular lipid droplets with 0.5% oil red O (Sigma-Aldrich, St. Louis, MO, USA).

Labeling of ADSCs With Green Fluorescent Protein

ADSCs were transfected with green fluorescent protein (pGFP-N; Clontech Laboratories [Takara Bio USA], Inc., Mountain View, CA, USA) by electroporation (Invitrogen™ Neon™ Transfection System, Thermo Fisher Scientific, Branchburg, NJ, USA), following the instructions provided by the manufacturer. After the first 48 h of culturing in L-DMEM supplemented with 10% FBS, the transformed cells were selected with G418 (200 mg/mL) under standard culture conditions. The selection of GFP-positive cells was maintained by culturing in the same medium supplemented with G418 (200 mg/mL) for three passages.

Detection of GFP-Positive ADSCs in Cardiac Tissue

GFP-labeled ADSCs, used for cell tracking after injection, were double-stained in sections for GFP and the antigen of interest. The slides were deparaffinized in cycles of xylene for 5 min each and rehydrated in a series of graded ethanol solutions. Antigen retrieval of the sections was performed using a steamer-citrate buffer antigen retrieval method. Endogenous peroxidase was inhibited by incubation with fresh 3% H_2O_2 in PBS. Nonspecific staining was blocked with a mixture of two serums (with respect to the type of antibodies used for blotting) in 1.5% PBS for 30 min at room temperature. Afterward, the sections were incubated in the mixture of two primary an-

tibodies in a pairwise fashion against GFP (Santa Cruz Biotechnology, Santa Cruz, CA, USA, catalog no: sc-9996 or sc-5385), desmin (Santa Cruz Biotechnology, Santa Cruz, CA, USA, catalog no: SC-23879), tropomyosin (Thermo Fisher Scientific, Branchburg, NJ, USA, catalog no: MS-1256-P), troponin T (Thermo Fisher Scientific, Branchburg, NJ, USA, catalog no: MS-295-P), and VEGF (Abcam, Cambridge, UK, catalog no: ab1316) for 1 h at room temperature. The sections were incubated in a mixture of two appropriate fluorescent conjugated secondary antibodies and mounted with mounting medium containing 4,6-diamidino-2-phenylindole (Santa Cruz Biotechnology, Santa Cruz, CA, USA). The cells were investigated under a fluorescence microscope (Zeiss Axio Observer 1, Carl Zeiss Microscopy GmbH, Jena, Germany).

Statistical Analysis

Data are presented as mean ± SD. Paired sample *t*-tests were used to compare differences in measurements (baseline and post-MI; post-MI and post-treatment) between pairs of groups. One-way ANOVA with least significant difference post-hoc analysis was performed to compare differences between the three groups. $p<0.05$ was considered statistically significant. All the statistical analyses were performed using IBM SPSS Statistics V 20 (Chicago, IL, USA).

Results

Characterization of ADSCs

Isolated cells from adipose tissue distributed sparsely on the culture flasks and displayed a mostly fibroblast-like and spindle-shaped morphology during the early days of incubation. In the later passages, most of these MSCs exhibited a large, flattened, or fibroblast-like morphology (Figure 1A-D). The immunophenotypic properties of ADSCs were determined by flow cytometry. Predefined markers that specify MSCs were used to define the characteristics of cultured cells. ADSCs expressed all MSC markers, including CD44, CD90, CD105, and MHC class I, but not CD45 or MHC class II (Figure 1E). Characterization studies of ADSCs, using immunofluorescent markers (**Supplementary Data 1**) and immunohistochemical (**Supplementary Data 2**) analysis, showed that they expressed various myogenic, osteogenic, and neurogenic stem cell markers. We studied the potential of ADSCs to differentiate into osteocytes and adipocytes (**Supplementary Data 3**). According to the morphological, histological, and immunohistochemical analysis, the cells were observed to differentiate successfully into various cell types.

Histological evaluations

Hematoxylin-eosin staining of the tissue sections from the infarct zones demonstrated pronounced fibrotic scar formation in the PBS (placebo) group. In the slides from the ADSC group, cardiomyocyte formations in the infarcted regions were detected (Figure 2).

Desmin, tropomyosin, troponin T, and GFP staining in tissue sections of the infarcted areas showed a prominent loss of muscle mass in the PBS group. In the ADSC group, GFP-tagged stem cells showed differentiation into cardiomyocytes at the infarct regions (Figures 3, 4, and 5). The ADSC group showed new vessel formation at the infarct sites in VEGF and GFP staining (Figure 6). Vascular density (number of vessels/inch^2) was significantly higher in the ADSC group compared to the PBS group ($p<0.001$, Figure 7). The infarct size was found to be significantly reduced in the ADSC group compared to the PBS group ($p<0.05$, Figure 8).

Follow-up

No mortality occurred in the sham-operated group (n=5). Four rabbits (40%) in the placebo group (n=10) were lost during the follow-up period after PBS injections (three were lost in the second week, and one in the third week following PBS injections). Only one rabbit (10%) was lost during the second week of follow-up after ADSC injection in the treatment group (n=10).

Deaths during the follow-up period were excluded from the study. Functional outcome analyses were performed on five animals in the sham-operated group, six in the placebo (PBS) group, and nine in the ADSC-injected treatment group.

LV Function

Initial echocardiographic measurements of the subjects did not differ significantly between the three study groups (EF [mean square: 1.36, df: 2, F: 1.12, $p=0.349$]; FS [mean square: 0.84, df: 2, F: 1.17, $p=0.334$]; LVIDd [mean square: 0.002, df: 2, F: 0.1, $p=0.905$]; LVIDs [mean square: 0.001, df: 2, F: 0.077, $p=0.926$]).

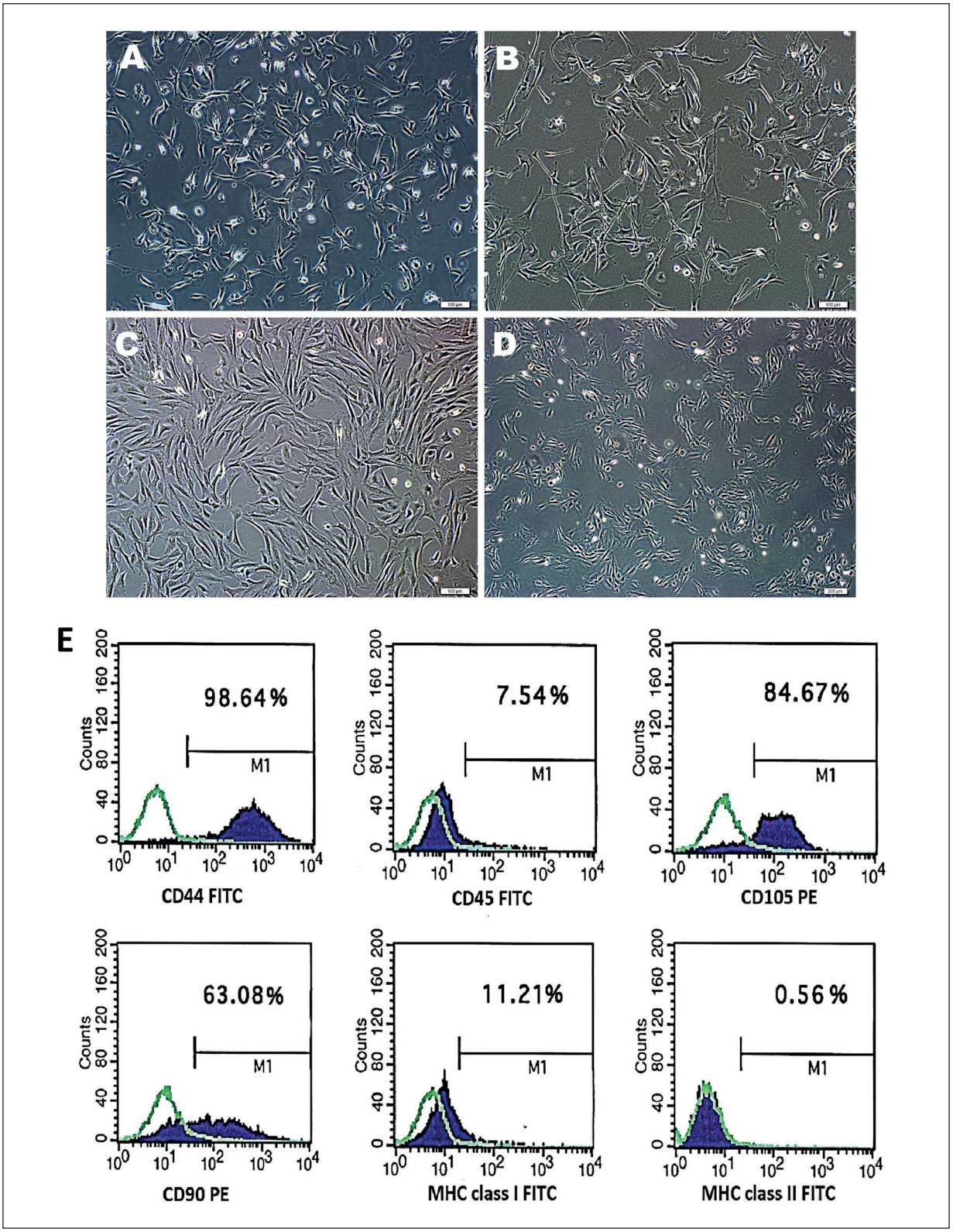

Figure 1. Phase-contrast microscopic images of AD-MSCs obtained from rabbit adipose tissue **(A,B,C,D)**. (A: P0 Day 4; B: P1 Day 3; C: P2 Day 3; D:P3 Day 2). (Scale bars: A-B-C:100 µm ve D:200 µm). Immunophenotypic characteristics of MSCs isolated from rabbit adipose tissue (P3) determined by flow cytometry analysis **(E)**. CD44, CD45, CD105, CD90, MHC class I and MHC class II markers are analyzed.

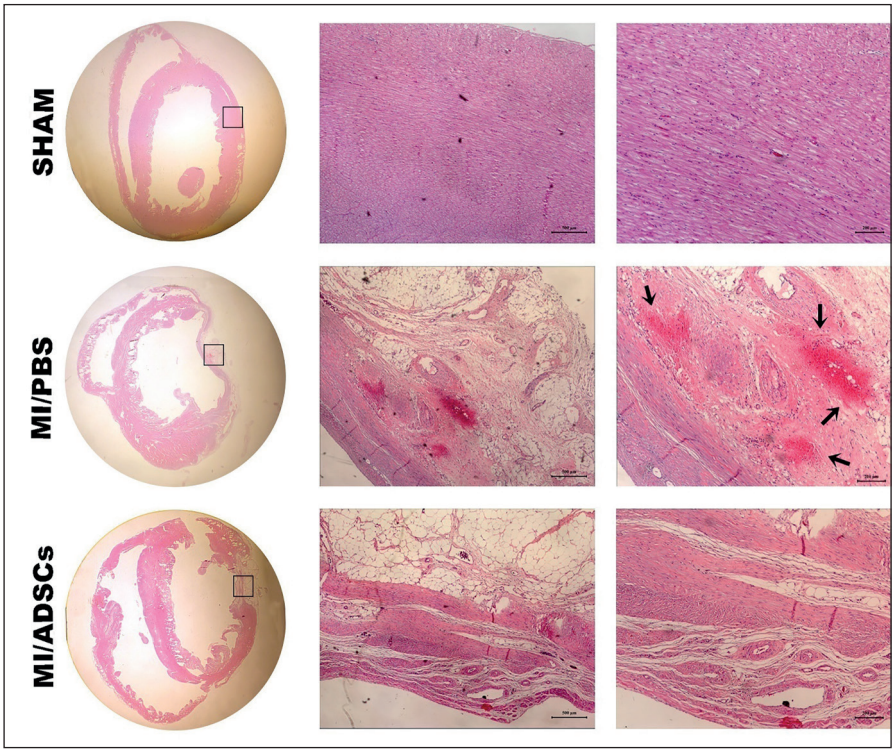

Figure 2. Hematoxylin eosin staining on tissue sections of all groups. Sham group tissue sections have normal cardiac tissue morphology. The MI/PBS group images show the infarct area with thinned left ventricular wall. In the tissue sections of MI/ADSCs group, it was observed that the tissue began to resemble normal heart tissue. (Hematoxylin is an alkaline pH dyestuff that staines cell nuclei and calcium deposits (blue). Eosin stains structures such as cytoplasm, protein accumulation, amyloid (pink)).

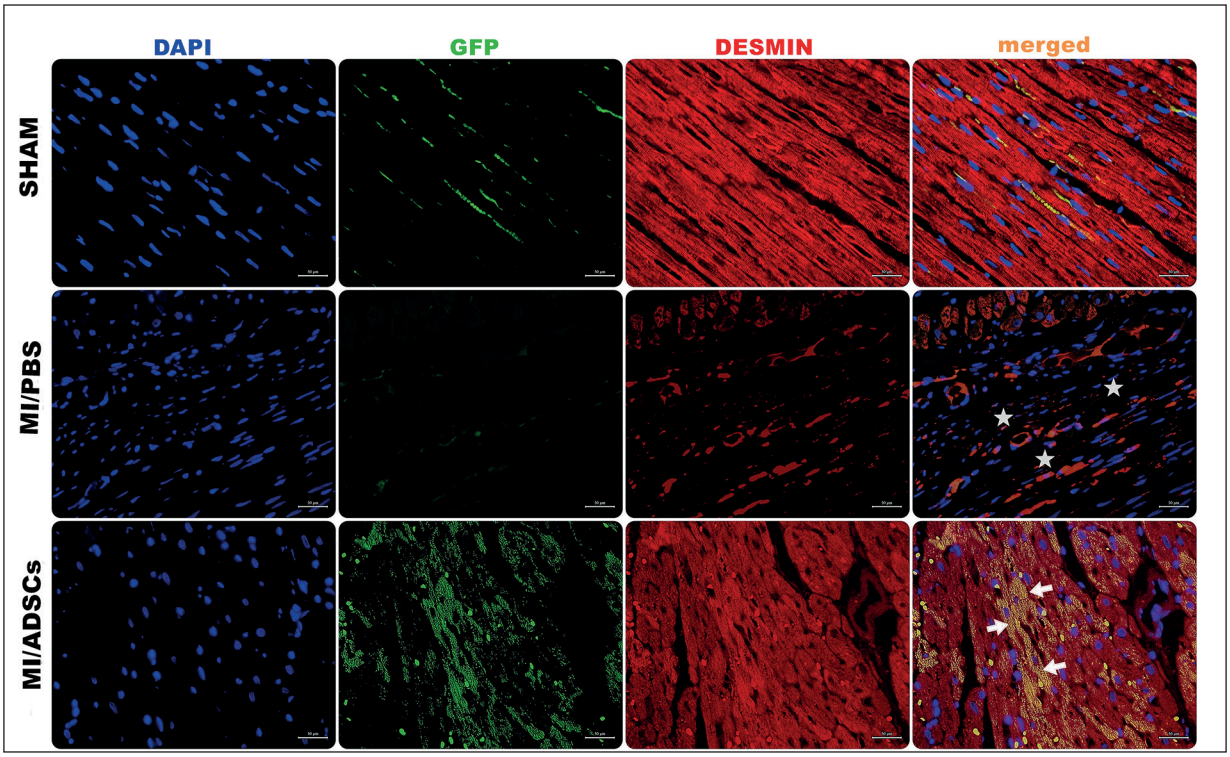

Figure 3. Desmin and GFP staining in tissue sections from rabbit heart tissues in all groups. While no abnormalities were observed in tissue sections of Sham group, muscle cell losses were observed in tissue sections of MI/PBS group (stars). In tissue sections of MI/ ADSCs group, it is seen that GFP $^{+}$ cells differentiate into muscle cells by placing GFP $^{+}$ cells at the damage site (white arrows). In the MSC group, the infarct area was decreased, filled with cells and appeared similar to the sham group (Blue:DAPI, Green:GFP, Red: Desmin). (Scale bars: 50 mm). (In the sham and MI/PBS group, erythrocytes were autofluorescent stained).

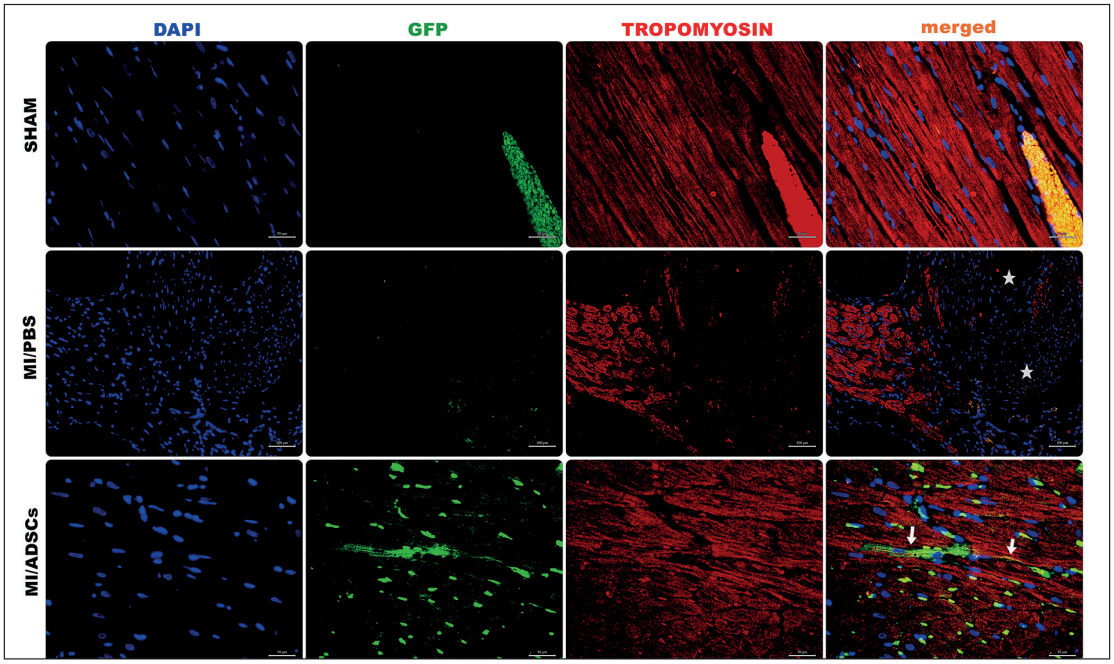

Figure 4. Tropomyosin and GFP staining in tissue sections from rabbit heart tissues in all groups. Tissue sections of the Sham group appear to be normal heart tissue. In MI/PBS group, the decrease in muscle mass is apparent, along with deposition of fat cells (star). The presence of Tropomyosin and GFP positive stained cells suggest differentiation of GFP + cells into cardiac muscle cells in MI/ADSCs group sections. Arrows point out overlapping GFP and Tropomyosin positive cells. (Blue:DAPI, Green:GFP, Red: VEGF). (Scale bars: 50 mm, 100 mm). (In the sham and MI/PBS group, erythrocytes were autofluorescent stained).

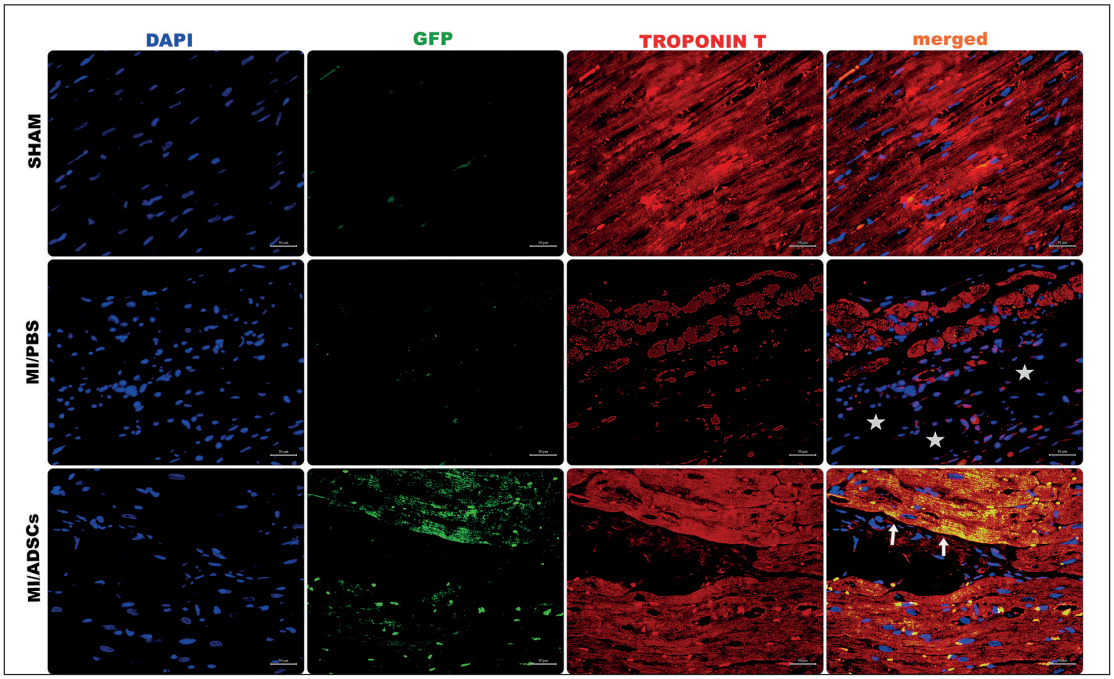

Figure 5. Troponin T and GFP staining in tissue sections from rabbit heart tissues in all groups. Tissue sections of the Sham group appear to be normal heart tissue. Muscle cells are decreased in the MI/PBS group tissue sections and clusters of fat cells are seen (star). In tissue sections of MI/ADSCs group, it is seen that GFP $^{+}$ cells differentiate into muscle cells by placing GFP $^{+}$ cells at the damage site (white arrow). (Blue:DAPI, Green:GFP, Red: Troponin T). (Scale bars: 50 mm). (In the sham and MI/PBS group, erythrocytes were autofluorescent stained).

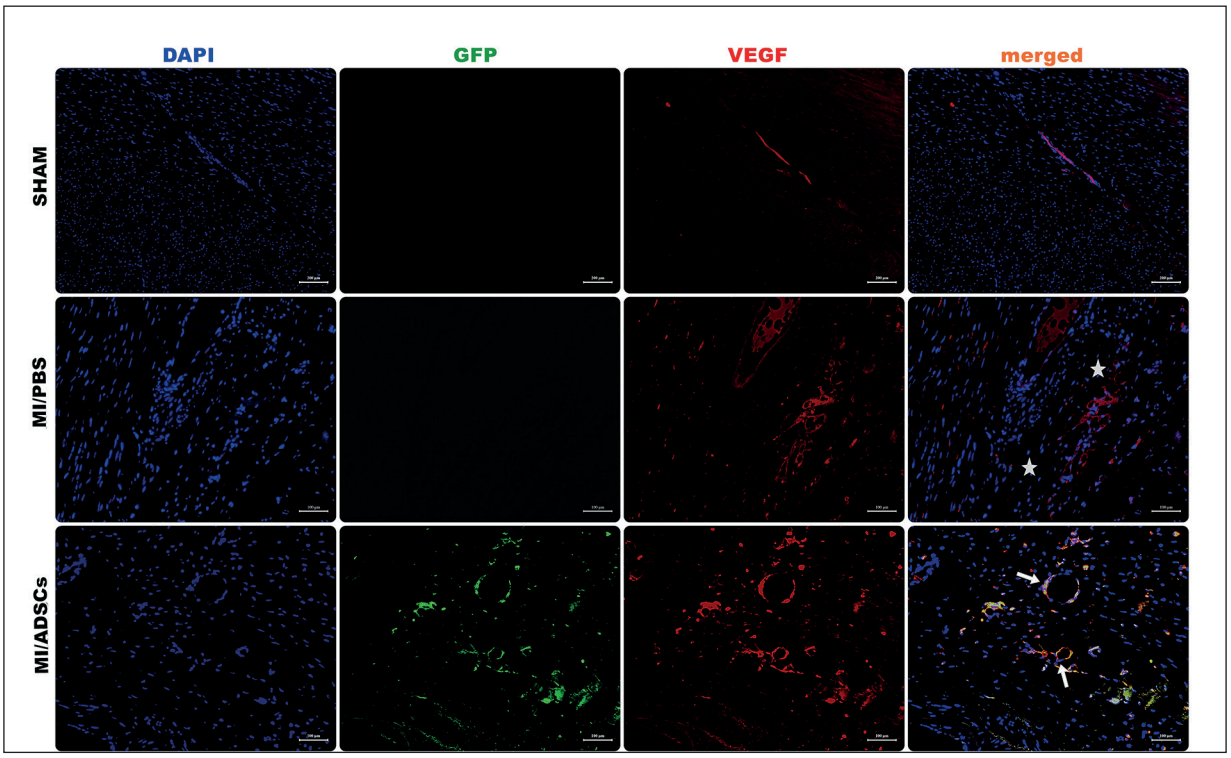

Figure 6. VEGF and GFP staining in tissue sections from rabbit heart tissues in all groups. Tissue sections of the Sham group appear to be normal heart tissue. In MI group, muscle cell density is decreased. The damaged area is devoid of vascular structures (star). MI/ADSCs group showed that GFP^+ cells differentiated into muscle cells at the site of injury. Overlapping VEGF and GFP positive cells indicate sites of new vessel formations in the damaged area (white arrows). (Blue:DAPI, Green:GFP, Red: VEGF). (Scale bars: 100 mm). (In the sham and MI/PBS group, erythrocytes were autofluorescent stained).

No significant changes were found in baseline EF in the sham-operated animals 1 month after the first operation (95% CI: -0.57, 0.61, p=0.930) or the second operation (95% CI: -0.69, 1.53, p=0.354; Table I).

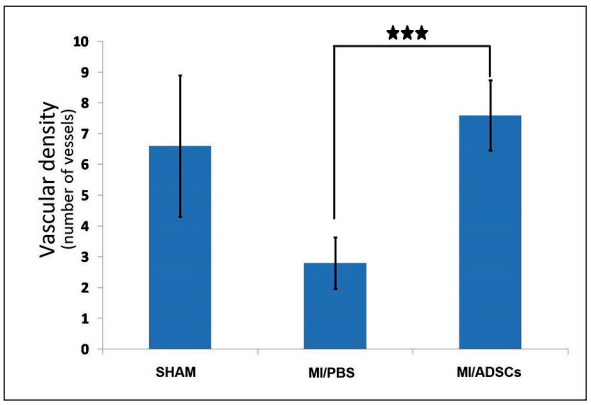

Figure 7. Comparative results of vascular density between SHAM, MI/PBS and MI/ADSCs groups. Vascular density was significantly increased in the treatment group compared to the placebo (p<0.001).

In the echocardiography controls following the first operation (induction of MI), animals in both the placebo and ADSC treatment groups showed significant reductions in EF (95% CI: 9.01, 14.89, p=0.0001; 95% CI: 10.96, 13.46, p<0.0001, respectively) and FS (95% CI: 6.14, 10.06, p=0.0001; 95% CI: 7.8, 9.62, p<0.0001, respectively) and

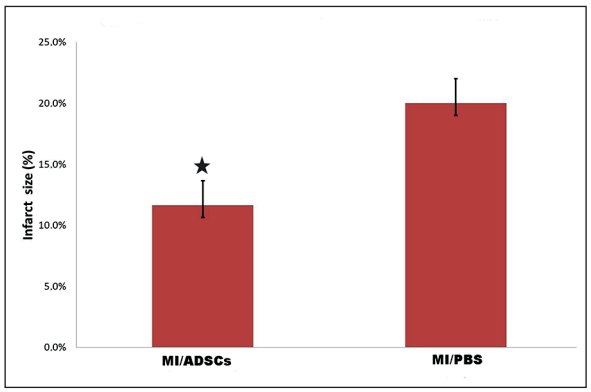

Figure 8. Comparative results of infarct size between MI/PBS and MI/ADSCs group (p <0.05).

Table I. Summary of echocardiographic functional study data.

					p-value	
	Groups	*Baseline*	*Post MI*	*Treatment*	p^{1}*	p^{2}**
EF (%, mean ± SD)	Sham	70.34 ± 1.62	70.32 ± 1.60	69.90 ± 1.75	0.930	0.354
	PBS	69.4 ± 1.0	57.45 ± 2.46	54.06 ± 2.24	0.0001	0.000085
	ADSC	70.07 ± 0.79	57.86 ± 1.75	62.53 ± 1.43	< 0.0001	< 0.0001
FS (%)	Sham	36.5 ± 1.37	36.64 ± 1.11	36.24 ± 1.29	0.567	0.223
	PBS	35.76 ± 0.68	27.66 ± 1.55	25.65 ± 1.34	0.0001	0.0001
	ADSC	36.31 ± 0.54	27.60 ± 0.96	31.0 ± 1.02	< 0.0001	0.00001
LVIDd (mm)	Sham	1.51 ± 0.16	1.50 ± 0.10	1.51 ± 0.12	0.884	1.0
	PBS	1.48 ± 0.14	1.56 ± 0.13	1.62 ± 0.11	0.0019	0.014
	ADSC	1.48 ± 0.11	1.59 ± 0.13	1.54 ± 0.12	0.00013	0.006
LVIDs (mm)	Sham	0.96 ± 0.11	0.95 ± 0.08	0.96 ± 0.09	0.812	0.711
	PBS	0.95 ± 0.09	1.12 ± 0.09	1.21 ± 0.09	0.000005	0.0014
	ADSC	0.94 ± 0.07	1.15 ± 0.09	1.06 ± 0.07	< 0.0001	0.000001

ADSC = Adipose tissue derived stem cells, EF = Ejection Fraction, FS = Fractional Shortening, LVIDd = Left ventricular internal diameter end diastole, LVIDs = Left ventricular internal diameter end systole, MI = myocardial infarction, PBS = Phosphate buffer saline. *Analysis between baseline and post-MI data. **Analysis between post-MI and treatment data.

significant increases in LVIDd (95% CI: -0.11, -0.04, p=0.0019; 95% CI: -0.14, -0.07, p=0.00013, respectively) and LVIDs (95% CI: -0.19, -0.15, p=0.000005; 95% CI: -0.23, -0.18, p<0.0001, respectively) from baseline, confirming the efficacy of the MI model used (Table I).

Following the second operation (ADSC treatment *vs.* placebo), monthly echocardiographic examination found, in contrast to previous post-MI measurements, a mean 4.7% increase in EF (95% CI: 5.22, 4.11, p<0.0001), 3.4% increase in FS (95% CI: 4.23, 2.57, p=0.000012), 0.04-mm decrease in LVIDd (95% CI: -0.016, -0.07, p=0.006), and 0.08-mm decrease in LVIDs (95% CI: -0.07, -0.097, p=0.000001) in the ADSC treated group, showing promising recovery. The efficacy of ADSC treatment was further supported by the ineffective treatment in the placebo group, which resulted in a further mean 3.4% decrease in EF (95% CI: -2.63, -4.14, p=0.000085), 2.02% decrease in FS (95% CI: -1.55, -2.49, p=0.000108), 0.07-mm increase in LVIDd (95% CI: 0.11, 0.19, p=0.014), and 0.08-mm increase in LVIDs (95% CI: 0.11, 0.047, p=0.001; Table I, Figure 9).

Discussion

Allogenic epicardial ADSCs were used for myocardial tissue regeneration by intramyocardial application in the peri-infarcted regions in this study. We focused on epicardial ADSCs as a valuable therapeutic option in tissue rescue and repair, based on their pro-angiogenetic and anti-apoptotic factor secretion, immunomodulatory effects, and capacity for multi-lineage differentiation and ready expansion[7,14]. It has been previously reported[15] that ADSCs have directly differentiated into cardiomyocytes *in vitro*. Most of the *in vivo* studies on stem cells derived from various adipose tissue sources have demonstrated that only a small fraction contributed to cardiomyocyte differentiation[16,17]. Epicardial ADSCs have different characteristics than other adipose tissue sources, having

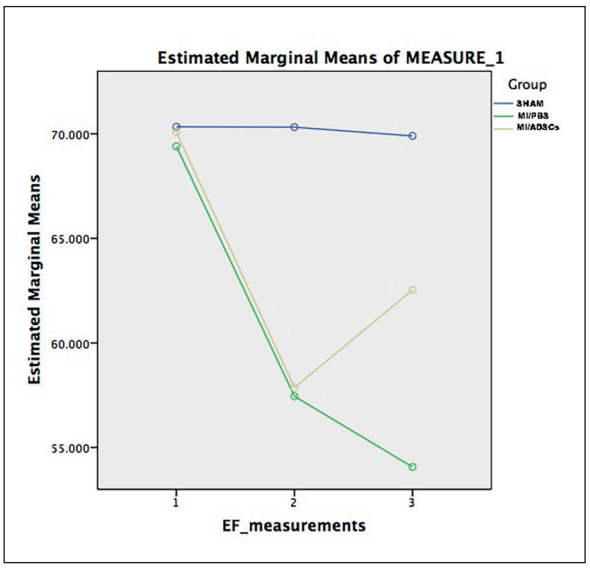

Figure 9. Changes in ejection fraction (EF, %) in each group. Significant remodeling effect of MSC treatment, reflected as increasing EF, while the MI/PBS group's EF continue to decrease.

more capacity to differentiate into cardiomyocytes[7]. GFP-tagged epicardial ADSCs used in this study presented desmin- and tropomyosin-positivity in the infarcted regions, demonstrating their cardiomyocyte differentiation potency.

MI is the leading cause of morbidity and mortality worldwide[18], and HF as a consequence of MI is a major issue of concern. Myocardial fibrosis due to MI is an important mechanism of cardiac remodeling that leads to HF. Recently, many researchers have focused their attention on treatments to decrease myocardial injury and fibrosis more effectively. The belief that the heart is a postmitotic organ and cannot regenerate itself has been challenged by numerous animal trials demonstrating that under ischemic stress conditions, cascades of repair mechanisms begin in the heart tissue[19]. To promote regeneration mechanisms under stress conditions, both transdifferentiation and especially paracrine signaling play major roles. Various stem cells have been studied to analyze the therapeutic results in infarcted heart tissue. There are multiple observations about the regenerative effect of pluripotent stem cells, but teratoma risk and ethical concerns restrict their clinical use[20]. Recently, several studies[10,21,22] have reported that human ADSCs revealed a higher capacity to reduce the infarct area in rat MI models compared to bone marrow–derived stem cells. In our study, we used ADSCs derived from epicardial fat due to their higher cardiomyogenic potential and lower adipogenic potential, as demonstrated in previous studies[7]. Experimental trials have demonstrated that epicardial fat has more ability to differentiate into cardiomyocytes due to brown adipose tissue characteristics[23,24]. ADSCs are also significantly less immunogenic than other cell types, allowing allogeneic transplantation[25]. Taking into account these findings, we decided to study epicardial ADSCs in a rabbit model of chronic myocardial ischemia.

Human progenitor cells derived from cardiac adipose tissue can differentiate toward endothelial cell lineages *in vivo*[10]. In our study, we detected VEGF in epicardial ADSCs and found a significant increase in vascular density in the ADSC treatment group. This clearly demonstrates the neo-angiogenic potential of these cells. The question of whether this angiogenic activity is a result of direct differentiation or a paracrine signaling effect merits further attention.

We analyzed the recovery of dynamic ventricular functions with echocardiography. EF measurements in the placebo group continued decreasing, as commonly observed in chronic myocardial ischemia due to cardiac remodeling. Conversely, a clinically significant increase in EF was observed in the epicardial ADSC treatment group. Our histologic evaluations also confirmed new cardiomyocyte formation in the ADSC treatment group, which contributed to better functioning wall motions and reversed cardiac remodeling.

This study has one notable limitation. Viability studies such as cardiac MRI or PET scanning could not be used due to their unavailability for small animals in our country at the time. We had to rely solely on detailed echocardiographic examination data, performed by blinded experienced professionals. However, immunohistochemical analysis supported our hypothesis that epicardial ADSCs are a valuable stem cell source for cardiomyocyte transdifferentiation and regeneration in ischemic stress conditions.

We performed a long-term follow-up study in a model of MI and ischemia in rabbits. The fate of epicardial ADSCs, when administered directly into the ischemic myocardium, could be investigated over a longer time *in vivo*. Our results show that these cells responded well in an ischemic environment by differentiating into proper cell lines to reconstruct a viable myocardium.

Conclusions

This study demonstrates that epicardial adipose tissue is a rich source of stem cells, which can differentiate into cardiomyocytes and endothelial cells under ischemic conditions. The differentiation of epicardial ADSCs into functional cardiac cell lines resulted in the reversal of cardiac remodeling when implanted in the infarcted myocardium. Allogenic epicardial ADSCs are non-immunogenic and non-teratogenic, which makes them a valuable source for cardiac regenerative cell therapy.

Conflict of Interest

The Authors declare that they have no conflict of interests.

Funding Statement

This study was funded by our institution, and grant number 2011/16 was assigned with permission of our Local Ethics Committee for Animal Experiments.

References

1) Yoshida K, Gould KL. Quantitative relation of myocardial infarct size and myocardial viability by positron emission tomography to left ventricular ejection fraction and 3-year mortality with and without revascularization. J Am Coll Cardiol 1993; 22: 984-997.
2) Planat-Benard V, Silvestre JS, Cousin B, André M, Nibbelink M, Tamarat R, Clergue M, Manneville C, Saillan-Barreau C, Duriez M, Tedgui A, Levy B, Pénicaud L, Casteilla L. Plasticity of human adipose lineage cells toward endothelial cells: physiological and therapeutic perspectives. Circulation 2004; 109: 656-663.
3) Portalska KJ, Leferink A, Groen N, Fernandes H, Moroni L, van Blitterswijk C, de Boer J. Endothelial differentiation of mesenchymal stromal cells. PLoS One 2012; 7: e46842.
4) Mizuno H, Zuk PA, Zhu M, Lorenz HP, Benhaim P, Hedrick MH. Myogenic differentiation by human processed lipoaspirate cells. Plast Reconstr Surg 2002; 109: 199-209.
v5) Dominici M, Le Blanc K, Mueller I, Slaper-Cortenbach I, Marini FC, Krause DS, Deans RJ, Keating A, Prockop DJ, Horwitz EM. Minimal criteria for defining multipotent mesenchymal stromal cells. The International Society for Cellular Therapy position statement. Cytotherapy 2006; 8: 315-317.
6) Nagata H, Ii M, Kohbayashi E, Hoshiga M, Hanafusa T, Asahi M. Cardiac adipose-derived stem cells exhibit high differentiation potential to cardiovascular cells in C57BL/6 mice. Stem Cells Transl Med 2016; 5: 141-151.
7) Wystrychowski W, Patlolla B, Zhuge Y, Neofytou E, Robbins RC, Beygui RE. Multipotency and cardiomyogenic potential of human adipose-derived stem cells from epicardium, pericardium, and omentum. Stem Cell Res Ther 2016; 7: 84.
8) Vuille C, Weyman AE. Left ventricle I: General considerations, assessment of chamber size and function. In: Weyman AE, editor. Principles and Practice of Echocardiography. 2nd edition. Philadelphia, PA, Lea & Febiger, 1994; pp. 575-624.
9) Hu N, Straub CM, Garzarelli AA, Sabey KH, Yockman JW, Bull DA. Ligation of the left circumflex coronary artery with subsequent MRI and histopathology in rabbits. J Am Assoc Lab Anim Sci 2010; 49: 838-844.
10) Bayes-Genis A, Soler-Botija C, Farré J, Sepúlveda P, Raya A, Roura S, Prat-Vidal C, Gálvez-Montón C, Montero JA, Büscher D, Izpisúa Belmonte JC. Human progenitor cells derived from cardiac adipose tissue ameliorate myocardial infarction in rodents. J Mol Cell Cardiol 2010; 49: 771-780.
11) Izmirli HH, Alagoz MS, Gercek H, Eren GG, Yucel E, Subasi C, Isgoren S, Muezzinoglu B, Karaoz E. Use of adipose-derived mesenchymal stem cells to accelerate neovascularization in interpolation flaps. J Craniofac Surg 2016; 27: 264-271.
12) Hamdi H, Planat-Benard V, Bel A, Puymirat E, Geha R, Pidial L, Nematalla H, Bellamy V, Bouaziz P, Peyrard S, Casteilla L, Bruneval P, Hagège AA, Agbulut O, Menasché P. Epicardial adipose stem cell sheets results in greater post-infarction survival than intramyocardial injections. Cardiovasc Res 2011; 91: 483-491.
13) Karaoz E, Aksoy A, Ayhan S, Sariboyaci AE, Kaymaz F, Kasap M. Characterization of mesenchymal stem cells from rat bone marrow: ultrastructural properties, differentiation potential and immunophenotypic markers. Histochem Cell Biol 2009; 132: 533-546.
14) Rehman J, Traktuev D, Li J, Merfeld-Clauss S, Temm-Grove CJ, Bovenkerk JE, Pell CL, Johnstone BH, Considine RV, March KL. Secretion of angiogenic and antiapoptotic factors by human adipose stromal cells. Circulation 2004; 109: 1292-1298.
15) Planat-Bénard V, Menard C, André M, Puceat M, Perez A, Garcia-Verdugo JM, Pénicaud L, Casteilla L. Spontaneous cardiomyocyte differentiation from adipose tissue stroma cells. Circ Res 2004; 94: 223-229.
16) Chang JC, Lee PC, Lin YC, Lee KW, Hsu SH. Primary adipose-derived stem cells enriched by growth factor treatment improves cell adaptability toward cardiovascular differentiation in a rodent model of acute myocardial infarction. J Stem Cells 2011; 6: 21-37.
17) Wang L, Deng J, Tian W, Xiang B, Yang T, Li G, Wang J, Gruwel M, Kashour T, Rendell J, Glogowski M, Tomanek B, Freed D, Deslauriers R, Arora RC, Tian G. Adipose-derived stem cells are an effective cell candidate for treatment of heart failure: an MR imaging study of rat hearts. Am J Physiol Heart Circ Physiol 2009; 297: H1020-H1031.
18) Mozaffarian D, Benjamin EJ, Go AS, Arnett DK, Blaha MJ, Cushman M, de Ferranti S, Després JP, Fullerton HJ, Howard VJ, Huffman MD, Judd SE, Kissela BM, Lackland DT, Lichtman JH, Lisabeth LD, Liu S, Mackey RH, Matchar DB, McGuire DK, Mohler ER 3rd, Moy CS, Muntner P, Mussolino ME, Nasir K, Neumar RW, Nichol G, Palaniappan L, Pandey DK, Reeves MJ, Rodriguez CJ, Sorlie PD, Stein J, Towfighi A, Turan TN, Virani SS, Willey JZ, Woo D, Yeh RW, Turner MB; American Heart Association Statistics Committee and Stroke Statistics Subcommittee. Heart disease and stroke statistics—2015 update: a report from the American Heart Association. Circulation 2015; 131: e29-e322.
19) Beltrami AP, Urbanek K, Kajstura J, Yan SM, Finato N, Bussani R, Nadal-Ginard B, Silvestri F, Leri A, Beltrami CA, Anversa P. Evidence that human cardiac myocytes divide after myocardial infarction. N Engl J Med 2001; 344: 1750-1757.
20) Nussbaum J, Minami E, Laflamme MA, Virag JA, Ware CB, Masino A, Muskheli V, Pabon L, Reinecke H, Murry CE. Transplantation of undifferentiated murine embryonic stem cells in the

heart: teratoma formation and immune response. FASEB J 2007; 21: 1345-1357.

21) Rasmussen JG, Frøbert O, Holst-Hansen C, Kastrup J, Baandrup U, Zachar V, Fink T, Simonsen U. Comparison of human adipose-derived stem cells and bone marrow-derived stem cells in a myocardial infarction model. Cell Transplant 2014; 23: 195-206.

22) Paul A, Srivastava S, Chen G, Shum-Tim D, Prakash S. Functional assessment of adipose stem cells for xenotransplantation using myocardial infarction immunocompetent models: comparison with bone marrow stem cells. Cell Biochem Biophys 2013; 67: 263-273.

23) Yamada Y, Wang XD, Yokoyama S, Fukuda N, Takakura N. Cardiac progenitor cells in brown adipose tissue repaired damaged myocardium. Biochem Biophys Res Commun 2006; 342: 662-670.

24) Liu Z, Wang H, Zhang Y, Zhou J, Lin Q, Wang Y, Duan C, Wu K, Wang C. Efficient isolation of cardiac stem cells from brown adipose. J Biomed Biotechnol 2010; 2010: 104296.

25) Strem BM, Hicok KC, Zhu M, Wulur I, Alfonso Z, Schreiber RE, Fraser JK, Hedrick MH. Multipotential differentiation of adipose tissue-derived stem cells. Keio J Med 2005; 54: 132-141.